Universitat de Barcelona

Master Thesis

OBLIQUE CORRECTIONS IN THE DINE-FISCHLER-SREDNICKI-ZHITNITSKY AXION MODEL

Author:
Alisa Katanaeva

Supervisor:
Prof. Domènec Espriu

Universitat de Barcelona
Master in Astrophysics, Particle Physics and Cosmology

Barcelona
September 2015

Abstract

In the Minimal Standard Model (MSM) there is no degree of freedom for dark matter. There are several extensions of the MSM introducing a new particle - an invisible axion, which can be regarded as a trustworthy candidate at least for a part of the dark matter component. However, as it is extremely weakly coupled, it cannot be directly measured at the LHC. We propose to explore the electroweak sector indirectly by considering a particular model that includes the axion and deriving consequences that could be experimentally tested.

We discuss the Dine-Fischler-Srednicki-Zhitnitsky (DFSZ) model, which extends the two-Higgs doublet model with an additional Peccei-Quinn symmetry and leads to a physically acceptable axion. The non-linear parametrization of the DFSZ model is exploited in the generic case where all scalars except the lightest Higgs and the axion have masses at or beyond the TeV scale. We compute the oblique corrections and use their values from the electroweak experimental fits to put constraints on the mass spectrum of the DFSZ model.

Contents

CHAPTER 1

Introduction

In this thesis we reexamine the Dine-Fischler-Srednicki-Zhitnitsky (DFSZ) model. It is the two-Higgs doublet model (2HDM) containing an additional singlet, endowed with a Peccei-Quinn (PQ) symmetry. Introduction of the PQ symmetry in the Standard Model (SM) leads to the solution of the strong CP problem but induces the necessity of two doublets and the presence of an axion. The last becomes physically acceptable in the DFSZ model. From one point of view, the model includes a lot of new physics coming from the 2HDM. From another, an invisible axion is a possible candidate at least for a part of the dark matter. Both these reasons, as well as the interplay between the 2HDM content and the axion, make this model interesting to study.

The discovery of a Higgs-like particle with $m_h \sim 126$ GeV and the development of experiments now probing the predictions of the standard electroweak theory with sufficient accuracy impose the constraints on any potential new physics that might exist at higher energies. Nevertheless, there is still a room for a wide variety of the 2HDM scenarios. In the same time the introduction of an axion restricts the number of possibilities, making more rigorous the phenomenological consequences of the DFSZ model.

The structure of this master thesis is as follows. In Chapter 2 we discuss the basic structure and symmetries of the DFSZ model. In Chapter 3 we build the effective Lagrangian of the theory and produce its mass spectrum. Chapter 4 describes the so-called oblique correction which are used to parametrize possible departures from the SM; theoretical calculations and experimental bounds are provided. Finally, in Chapter 5 we observe the cases in which it is probable to have rather light spectra and find the experimentally allowed regions for the masses of new particles. Thus, our aim is to get the spectrum that can be tested at experiments in near future or, in other words, to predict new states in the TeV region.

CHAPTER 2

The Dine-Fischler-Srednicki-Zhitnitsky model

2.1 The two-Higgs-doublet model

There are three sectors of the Standard Model relevant to the electroweak interactions: gauge boson, fermion and scalar. While the fermion structure is rather complicated with many families and mixing, the scalar structure is assumed to be the simplest one - just one $SU(2)$ doublet.

Some restrictions on the scalar structure are commonly derived from the parameter ρ experimentally measured as [1]

$$\rho = 1.00040 \pm 0.00024. \tag{2.1}$$

At the tree-level it is defined as:

$$\rho \equiv \frac{M_W^2}{M_Z^2 \cos^2 \theta_W} \tag{2.2}$$

with θ_W the Weinberg angle and $M_W,\ M_Z$ the electroweak gauge boson masses. The ρ parameter is exactly 1 in the SM due to the custodial symmetry of Higgs potential (see Section 2.3). In the $SU(2) \times U(1)$ gauge theory, if there are n scalar multiplets ϕ_i, with weak isospin I_i, weak hypercharge Y_i, and vacuum expectation value (VEV) of the neutral components v_i, then the parameter ρ is, at tree level [2],

$$\rho = \frac{\sum\limits_{i=1}^{n} (I_i(I_i+1) - \frac{1}{4}Y_i^2) v_i}{\sum\limits_{i=1}^{n} \frac{1}{2} Y_i^2 v_i}. \tag{2.3}$$

From the equation (2.3) it is clear that both $SU(2)$ singlets and $SU(2)$ doublets give $\rho = 1$. Thus, the simplest way to extend the SM is to add new scalar doublets and singlets.

The two-Higgs-doublet model is the most popular extension in this direction. The best known motivation for studying 2HDMs is supersymmetry. In the Minimal Supersymmetric Standard Model (MSSM) it is impossible to give mass simultaneously to the charge $2/3$ and charge $-1/3$ quarks via the SM mechanism. The superpotential must be holomorphic and therefore cannot contain the Higgs field and its complex conjugate. Moreover, the cancellation of anomalies also requires that an additional doublet is added. Nevertheless, 2HDM can be also interesting on its own as a theory with reach phenomenology, including possibly (but not necessarily) flavour-changing neutral currents (FCNCs), custodial symmetry breaking terms or even new sources of CP violation.

Depending on the way that the two doublets couple to fermions, 2HDMs are classified as type I, II or III (see e.g. [2] for details), with different implications on the flavour sector. Type I and II 2HDMs can be made free from FCNC by the introduction of discrete symmetries.

Type III models have FCNC at tree level. They do not fit in the Paschos-Glashow–Weinberg theorem which in application to the SM implies that all right-handed quarks of a given charge must couple to a single Higgs multiplet.

For this work it is important that the presence of two Higgs doublets is a necessary element of the DFSZ model.

2.2 Peccei-Quinn symmetry and axions

Another distinguishing feature of the DFSZ model is the appearance of an axion. Peccei and Quinn [3] noted that a possible CP-violating term in the QCD Lagrangian, $\mathcal{L}_\theta = (\theta g_s^2/32\pi^2)F\tilde{F}$, can be rotated away if the Lagrangian contains a global $U(1)_{PQ}$ symmetry. This symmetry is necessarily spontaneously broken, and its introduction into the theory effectively replaces the static CP-violating angle θ with a dynamical CP-conserving field - the axion. The axion is the Nambu-Goldstone boson of the broken $U(1)_{PQ}$ Peccei-Quinn symmetry [4]. The order parameter associated with the breaking is called f_a. In the original Peccei-Quinn model it is required that there are two Higgs doublets and that the $U(1)_{PQ}$ symmetry breakdown coincides with that of electroweak breaking $f_a = v_F$, with $v_F \simeq 250$ GeV. The properties of such PQ axion can be determined with some confidence, and no such particle has been observed.

So, the original PQ model was long ago ruled out by experiment. Dine, Fischler and Srednicki [5] and Zhitnitsky [6] independently proposed a generalization of the Peccei-Quinn scheme with very light and very weakly coupled to ordinary matter, i.e. harmless, axion. All complication consists in addition of a scalar field that is a $SU(2) \times U(1)$ singlet and carries PQ charge. There is also another invisible axion model, the KSVZ model, introduced by Kim and Shifman, Vainshtein and Zakharov. For a detailed information about this model, as well as about axion cosmology and experimental searches an interested reader is referred to the review [7].

Here we survey the field content of the DFSZ model. To make the Standard Model invariant under a $U(1)_{PQ}$ transformation, one must introduce two Higgs fields to absorb independent chiral transformations of the up- and down-quarks (and leptons). So, we work with two Higgs doublets and a complex scalar singlet:

$$\phi_1 = \begin{pmatrix} \alpha_+ \\ \alpha_0 \end{pmatrix}; \quad \phi_2 = \begin{pmatrix} \beta_+ \\ \beta_0 \end{pmatrix}; \quad \phi. \tag{2.4}$$

The vevs of the fields are

$$\langle\phi_1\rangle = \begin{pmatrix} 0 \\ v_1 \end{pmatrix}; \quad \langle\phi_2\rangle = \begin{pmatrix} 0 \\ v_2 \end{pmatrix}; \quad \langle\phi\rangle = v_\phi. \tag{2.5}$$

We can define the usual electroweak vacuum expectation value as $v^2 = (v_1^2 + v_2^2)/2$ and the well-known 2HDM parameter $\tan\beta = v_2/v_1$. The DFSZ model includes a 2HDM of type II: ϕ_1 couples only to right-handed charge $2/3$ quarks, ϕ_2 couples only to the right-handed charge $-1/3$ quarks and to right-handed charged leptons. The Yukawa terms have the structure:

$$\mathcal{L}_Y = G_1 \bar{q}_L \tilde{\phi}_1 u_R + G_2 \bar{q}_L \phi_2 d_R + G_3 \bar{l}_L \phi_2 e_R + h.c., \tag{2.6}$$

and similarly for other quarks and leptons, here $\tilde{\phi}_i = i\tau_2 \phi_i^*$.

The Lagrangian should possess a global symmetry at the classical level. The corresponding PQ transformation acts on the scalars as

$$\phi_1 \to e^{iX_1\theta}\phi_1, \quad \phi_2 \to e^{iX_2\theta}\phi_2, \quad \phi \to e^{iX_\phi\theta}\phi \tag{2.7}$$

and on the fermions as

$$q_L \to q_L, \quad l_L \to l_L, \quad u_R \to e^{iX_u\theta}u_R, \quad d_R \to e^{iX_d\theta}d_R, \quad e_R \to e^{iX_e\theta}e_R. \tag{2.8}$$

For the Yukawa terms to be PQ-invariant we need

$$X_u = X_1, \quad X_d = -X_2, \quad X_e = -X_2. \tag{2.9}$$

For the potential we choose the one respecting CP, $SU(2)\times U(1)$ and $U(1)_{PQ}$ symmetries:

$$\begin{aligned} V(\phi,\phi_1,\phi_2) \;=\; & \lambda_\phi(\phi^*\phi - V_\phi^2)^2 + \lambda_1(\phi_1^\dagger\phi_1 - V_1^2)^2 + \lambda_2(\phi_2^\dagger\phi_2 - V_2^2)^2 + \\ & +\lambda_3(\phi_1^\dagger\phi_1 - V_1^2 + \phi_2^\dagger\phi_2 - V_2^2)^2 + \\ & +\lambda_4\left[(\phi_1^\dagger\phi_1)(\phi_2^\dagger\phi_2) - (\phi_1^\dagger\phi_2)(\phi_2^\dagger\phi_1)\right] + \\ & +(a\phi_1^\dagger\phi_1 + b\phi_2^\dagger\phi_2)\phi^*\phi + c(\phi_1^\dagger\phi_2\phi^2 + \phi_2^\dagger\phi_1\phi^{*2}). \end{aligned} \tag{2.10}$$

Note that to maintain PQ invariance the condition $-X_1 + X_2 + 2X_\phi = 0$ coming from the c term should be fulfilled.

If we impose that the PQ current does not couple to the Goldstone boson that is eaten by the Z, we also get $X_1\cos^2\beta + X_2\sin^2\beta = 0$. If furthermore we choose $X_\phi = -\frac{1}{2}$ the PQ charges of the doublets are

$$X_1 = -\sin^2\beta, \quad X_2 = \cos^2\beta. \tag{2.11}$$

2.3 Custodial symmetry

Here we discuss another possible symmetry of the Lagrangian. One can note that in the SM with one Higgs doublet, $\Phi = \begin{pmatrix} \varphi_1 + i\varphi_2 \\ \varphi_3 + i\varphi_4 \end{pmatrix}$, the scalar potential only depends on $\Phi^\dagger\Phi = \varphi_1^2 + \varphi_2^2 + \varphi_3^2 + \varphi_4^2$. Therefore, the SM potential automatically has $SO(4)$ symmetry. The group $SO(4)$ is isomorphic to $SU(2)\times SU(2)$, which is larger than the SM gauge

Parameter	**Breaking of Custodial Symmetry**
λ_1	$\lambda + \lambda_B$
λ_2	$\lambda - \lambda_B$
λ_3	λ_3
λ_4	$2\lambda + \lambda_{4B}$
λ_ϕ	λ_ϕ
V_1^2	$V^2 + V_B^2$
V_2^2	$V^2 - V_B^2$
V_ϕ	V_ϕ
a, b	$a + a_B = b$
c	c

Table 2.1: Conditions on the parameters of the scalar potential demanded by the custodial symmetry. Exact custodial symmetry corresponds to all "B" parameters being zero.

group $SU(2)_L \times U(1)_Y$. When the Higgs field acquires the non-zero VEV this symmetry is broken to $SO(3)$ equivalent to $SU(2)$. On the other hand, this symmetry $SO(4)$ is respected neither by the scalar gauge-kinetic terms, specifically, those involving the weak-hypercharge coupling g', nor by the Yukawa terms, linear in Φ, since the up-type and down-type quarks have different masses. Thus, $SO(4)$ is not a symmetry of the full SM Lagrangian, rather a symmetry only of the scalar potential; it is usually regarded as an approximate symmetry, since in the scalar sector it is only broken by (small) g' terms in the kinetic energy, and called custodial symmetry. In the limit $g' \to 0$ $(\sin^2\theta_W \to 0)$ the gauge bosons have equal masses and form a triplet of the $SU(2)$ unbroken global symmetry. The experimental value of the ρ parameter (2.1) characterizes the breaking of the custodial symmetry, which manifests itself in keeping the equality $\rho = 1$ (2.2), even when $g' = 0$.

To make more evident such global symmetries of the potential of the DFSZ model one can introduce a matrix notation [8]. First, we construct the 2×2 matrices from the fields of Higgs doublets:

$$\Phi_{12} = (\tilde{\phi}_1\ \phi_2) = \begin{pmatrix} \alpha_0^* & \beta_+ \\ -\alpha_- & \beta_0 \end{pmatrix}, \quad \Phi_{21} = (\tilde{\phi}_2\ \phi_1) = \begin{pmatrix} \beta_0^* & \alpha_+ \\ -\beta_- & \alpha_0 \end{pmatrix} = \tau_2 \Phi_{12}^* \tau_2. \tag{2.12}$$

Secondly, we consider the following combinations:

$$I = \Phi_{12}^\dagger \Phi_{12} = \begin{pmatrix} \phi_1^\dagger \phi_1 & \tilde{\phi}_1^\dagger \phi_2 \\ -\phi_1^\dagger \tilde{\phi}_2 & \phi_2^\dagger \phi_2 \end{pmatrix}, \tag{2.13}$$

$$J = \Phi_{12}^\dagger \Phi_{21} = \begin{pmatrix} \phi_2^\dagger \phi_1 & 0 \\ 0 & \phi_2^\dagger \phi_1 \end{pmatrix}. \tag{2.14}$$

Their vevs are

$$\langle I \rangle = \begin{pmatrix} v_1^2 & 0 \\ 0 & v_2^2 \end{pmatrix}, \quad \langle J \rangle = v_1 v_2. \tag{2.15}$$

This vacuum is not invariant under the full group $SU(2)_L \times SU(2)_R$. However, if $v_1 = v_2$, then $\langle I\rangle$ is proportional to the 2×2 identity matrix and the vacuum preserves a group $SU(2)_V$ (the V stands for "vectorial"), corresponding to identical matrices, i.e. $L = R$. This remaining group preserved by the vacuum is the custodial-symmetry group. However, most authors refer to the potential invariant under $SU(2)_L \times SU(2)_R$ as displaying the custodial symmetry, and we will also employ this equivocal terminology.

The last thing is to define the constant matrix W,

$$W = (V_1^2 + V_2^2)\frac{\mathbf{I}}{2} + (V_1^2 - V_2^2)\frac{\tau_3}{2} = \begin{pmatrix} V_1^2 & 0 \\ 0 & V_2^2 \end{pmatrix}, \tag{2.16}$$

and then, the potential can be written as:

$$\begin{aligned} V(\phi, I, J) \;\; = \;\; & \lambda_\phi(\phi^*\phi - V_\phi^2)^2 + \frac{\lambda_1}{4}\left\{\mathrm{Tr}\left[(I-W)(1+\tau_3)\right]\right\}^2 + \\ & + \frac{\lambda_2}{4}\left\{\mathrm{Tr}\left[(I-W)(1-\tau_3)\right]\right\}^2 + \lambda_3\left[\mathrm{Tr}(I-W)\right]^2 + \\ & + \frac{\lambda_4}{4}\,\mathrm{Tr}\left[I^2 - (I\tau_3)^2\right] + \frac{1}{2}\,\mathrm{Tr}\left[(a+b)I + (a-b)I\tau_3\right]\phi^*\phi + \\ & + \frac{c}{2}\,\mathrm{Tr}(J\phi^2 + J^\dagger\phi^{*2}). \end{aligned} \tag{2.17}$$

A custodial global $SU(2)_L \times SU(2)_R$ transformation acts on our fields as

$$\Phi_{ij} \to L\Phi_{ij}R^\dagger, \quad I \to RIR^\dagger, \quad J \to J. \tag{2.18}$$

If $SU(2)_L \times SU(2)_R$ is to be a symmetry, the parameters of the potential have to be set according to the custodial relations in Table 1.1 (see also [9]). In the limit of custodial symmetry, all the "B" parameters vanish. In total, there are 11 parameters of which 7 are custodial preserving and 4 are custodial breaking.

Finally, let us establish the action of the PQ symmetry previously discussed in this parametrization. Under the PQ transformation:

$$\Phi_{12} \to \Phi_{12}e^{iX\theta}, \quad \phi \to e^{iX_\phi\theta}\phi \tag{2.19}$$

with

$$X = \frac{X_2 - X_1}{2}\mathbf{I} - \frac{X_2 + X_1}{2}\tau_3, \quad X_\phi = \frac{X_2 - X_1}{2}. \tag{2.20}$$

Using the value from Eqn. (2.11):

$$X = \begin{pmatrix} \sin^2\beta & 0 \\ 0 & \cos^2\beta \end{pmatrix}, \quad X_\phi = -\frac{1}{2}. \tag{2.21}$$

CHAPTER 3

Effective Lagrangian

3.1 General aspects of Effective Lagrangian technique

Firstly, consider that we have only the gauge and Goldstone bosons as the light degrees of freedom. The Goldstone bosons are collected into the unitarity matrix $\mathcal{U} = \exp\left(i\frac{\vec{G}\cdot\vec{\tau}}{v}\right)$, which is the building block of the Lagrangian. One constructs the most general Lagrangian with the desired symmetries via a derivative expansion:

$$\mathcal{L} = \mathcal{L}^2 + \mathcal{L}^4 + ..., \tag{3.1}$$

where the indices denote the dimensionality of the corresponding operators. This can also be written in the form of the Effective Chiral Lagrangian:

$$\mathcal{L} = \frac{v^2}{4}\operatorname{Tr} D_\mu \mathcal{U}^\dagger D^\mu \mathcal{U} + \sum_{i=0}^{13} a_i \mathcal{O}_i, \tag{3.2}$$

where the first term is universal, $\mathcal{O}_i$ is a set of local gauge invariant operators and D_μ is a covariant derivative. Coefficients a_i collect all information from integrated out heavy degrees of freedom including the effects of physics beyond the Standard Model. Of particular interest are the effective couplings corresponding to the following operators: the second independent $\mathcal{O}(p^2)$ one,

$$\mathcal{L}^2 = \frac{v^2}{4}\operatorname{Tr} D_\mu \mathcal{U}^\dagger D^\mu \mathcal{U} + a_0 \frac{v^2}{4}[\operatorname{Tr}(\tau_3 \mathcal{U}^\dagger D^\mu \mathcal{U})]^2, \tag{3.3}$$

and a couple of $\mathcal{O}(p^4)$ operators:

$$\mathcal{L}^4 = \frac{1}{2} a_1 g g' \operatorname{Tr}(\mathcal{U} B_{\mu\nu} \mathcal{U}^\dagger W^{\mu\nu}) - \frac{1}{4} a_8 g^2 \operatorname{Tr}(\mathcal{U}\tau_3\mathcal{U}^\dagger W_{\mu\nu}) \operatorname{Tr}(\mathcal{U}\tau_3\mathcal{U}^\dagger W^{\mu\nu}) + ... \tag{3.4}$$

In the last expression $B_{\mu\nu}$ and $W_{\mu\nu}$ are the field strength tensors associated to the $U(1)_Y$ and $SU(2)_L$ gauge fields.

3.2 The non-linear parametrization of the DFSZ model

The difference with the DFSZ model under consideration is that we have additional light particles – light Higgs boson h and axion a_ϕ. As we can clearly distinguish generically heavy states from the light ones it is natural to use a non-linear realization to describe the low energy sector.

We decompose the matrix-valued Φ_{12} field in the following form

$$\Phi_{12} = \mathcal{U}\mathcal{M}_{12}. \tag{3.5}$$

As in the previous section $\mathcal{U}$ is a 2×2 matrix containing the three Goldstone bosons G_i associated to the breaking of $SU(2)_L \times U(1)_Y$ to $U(1)_{em}$:

$$\mathcal{U} = \exp\left(i\frac{\vec{G}\cdot\vec{\tau}}{v}\right). \tag{3.6}$$

Note that the matrices I and J of Eq. (2.13), (2.14) entering the DFSZ potential are actually independent of $\mathcal{U}$. This is immediate to see in the case of I while for J one has to use the property $\tau_2\mathcal{U}^* = \mathcal{U}\tau_2$ valid for $SU(2)$ matrices. The effective potential then does depend only on the degrees of freedom contained in $\mathcal{M}_{12}$ whereas the Goldstone bosons drop from the potential, since, under a global $SU(2)_L \times SU(2)_R$ rotation, Φ_{12} and $\mathcal{U}$ transform as

$$\Phi_{12} \to L\Phi_{12}R^\dagger, \quad \mathcal{U} \to L\mathcal{U}R^\dagger \;\Rightarrow\; \mathcal{M}_{12} \to R\mathcal{M}_{12}R^\dagger. \tag{3.7}$$

There is also the singlet field in the scalar potential, it can be parametrized as:

$$\phi = \rho + iG_\phi. \tag{3.8}$$

The phase of ϕ does not drop from the potential automatically because of the c term. G_ϕ mixes with the usual 0^- scalar from the 2HDM. To have a well-defined massless state we need to find a suitable phase both in $\mathcal{M}_{12}$ and in ϕ that drops from the potential.

Let us write $\mathcal{M}_{12} = M_{12}U_a$, where U_a is a unitary matrix containing the axion. There is some freedom in choosing U_a, it can have the identity generator as well as the τ_3 one. To fix this we need to consider the gauge invariant kinetic term:

$$\mathcal{L}_{\text{kin}} = \frac{1}{2}(\partial_\mu\phi)^*\partial^\mu\phi + \frac{1}{4}\,\text{Tr}\left[(D_\mu\Phi_{12}^\dagger)D^\mu\Phi_{12}\right], \tag{3.9}$$

with the covariant derivative defined as:

$$D_\mu\Phi_{12} = \partial_\mu\Phi_{12} - i\frac{g}{2}\vec{W}_\mu\cdot\vec{\tau}\Phi_{12} + i\frac{g'}{2}B_\mu\Phi_{12}\tau_3. \tag{3.10}$$

If we define

$$U_a = \exp\left(i\frac{2a_\phi X}{\sqrt{v_\phi^2 + v^2\sin^2 2\beta}}\right), \quad X = \begin{pmatrix} \sin^2\beta & 0 \\ 0 & \cos^2\beta \end{pmatrix} \tag{3.11}$$

all terms in the kinetic term are diagonal and exhibit the canonical normalization. Moreover, the axion field a_ϕ is no longer in the potential. Note that the phase redefinition implied in U_a exactly coincides with the realization of the PQ symmetry on Φ_{12} ((2.19) - (2.21)). This identifies uniquely the axion degree of freedom.

Collecting everything aforementioned together, the non-linear parametrization of Φ_{12} reads as[1]

$$\Phi_{12} = \mathcal{U} M_{12} U_a, \tag{3.12}$$

with

$$M_{12} = \sqrt{2}\begin{pmatrix} (v+H)c_\beta - \left(S - \frac{iv_\phi}{\sqrt{v_\phi^2+v^2 s_{2\beta}^2}}\tilde{A}_0\right)s_\beta & \sqrt{2}H_+ c_\beta \\ \sqrt{2}H_- s_\beta & (v+H)s_\beta + \left(S + \frac{iv_\phi}{\sqrt{v_\phi^2+v^2 s_{2\beta}^2}}\tilde{A}_0\right)c_\beta \end{pmatrix} \tag{3.13}$$

where the field redefinition we use is as follows

$$v + H = \frac{c_\beta}{\sqrt{2}}\Re[\alpha_0] + \frac{s_\beta}{\sqrt{2}}\Re[\beta_0], \quad S = -\frac{s_\beta}{\sqrt{2}}\Re[\alpha_0] + \frac{c_\beta}{\sqrt{2}}\Re[\beta_0], \tag{3.14}$$

$$H_\pm = \frac{c_\beta \beta_\pm - s_\beta \alpha_\pm}{2}. \tag{3.15}$$

The singlet field is non-linearly parametrized as

$$\phi = \left(v_\phi + \rho - i\frac{v s_{2\beta}}{\sqrt{v_\phi^2 + v^2 s_{2\beta}^2}}\tilde{A}_0\right)\exp\left(i\frac{a_\phi}{\sqrt{v_\phi^2 + v^2 s_{2\beta}^2}}\right). \tag{3.16}$$

The fields of H, S and ρ are not mass eigenstates but they have vanishing vevs. The mass eigenstates are defined through the rotation matrix R (see Apendix A):

$$H = \sum_{i=1}^{3} R_{Hi} h_i, \quad S = \sum_{i=1}^{3} R_{Si} h_i, \quad \rho = \sum_{i=1}^{3} R_{\rho i} h_i. \tag{3.17}$$

H, S are also called interaction eigenstates. For instance, H has the same coupling to the gauge fields as the SM Higgs boson, but the Higgs mass $m_h \simeq 126$ GeV is attributed to the lightest of h_i states.

The construction of the effective Lagrangian for the DFSZ model goes the same way as described in the previous section. The difference is that we need to include additional light particles explicitly as dynamical states. The corresponding effective Lagrangian will be:

$$\begin{aligned} \mathcal{L} \;=\; & \frac{v^2}{4}\left(1 + 2g_1\frac{h}{v} + g_2\frac{h^2}{v^2} + ...\right)\mathrm{Tr}\,\mathcal{D}_\mu\mathcal{U}^\dagger\mathcal{D}^\mu\mathcal{U} + \\ & + \left(\frac{v_\phi^2}{v_\phi^2 + v^2\sin^2 2\beta}\right)\partial_\mu a_\phi \partial^\mu a_\phi + \frac{1}{2}\partial_\mu h \partial^\mu h - V(h) + \\ & + \sum_{i=0}^{13} a_i\left(\frac{h}{v}\right)\mathcal{O}_i + \mathcal{L}_{ren}, \end{aligned} \tag{3.18}$$

where

$$\mathcal{D}_\mu\mathcal{U} = D_\mu\mathcal{U} + \mathcal{U}(\partial_\mu U_a)U_a^\dagger,$$

[1] Here we introduce the short-hand notation $s_{m\beta}^n \equiv \sin^n(m\beta)$ and $c_{m\beta}^n \equiv \cos^n(m\beta)$.

$$V(h) = \frac{m_h^2}{2}h^2 - d_3(\lambda v)h^3 - d_4\frac{\lambda}{4}h^4,$$
$$\mathcal{L}_{ren} = \frac{c_1}{v^4}(\partial_\mu h\partial^\mu h)^2 + \frac{c_2}{v^2}\,\mathrm{Tr}\,\mathcal{D}_\mu\mathcal{U}^\dagger\mathcal{D}^\mu\mathcal{U} + \frac{c_3}{v^2}(\partial_\mu h\partial^\nu h)\,\mathrm{Tr}\,\mathcal{D}^\mu\mathcal{U}^\dagger\mathcal{D}_\nu\mathcal{U}. \quad (3.19)$$

The terms in $\mathcal{L}_{ren}$ are required for renormalizability [10] at the one-loop level and play no role in the discussion. The couplings a_i are now functions of h/v and can be regularly expanded. The constant parts $a_i(0)$ correspond to the coefficients in Eqn. (3.3), (3.4) and are related to the electroweak precision parameters.

3.3 Mass eigenstates

Having defined the fields we proceed with the description of the mass spectrum of the model (following the work [11]). We have two doublets and a singlet, so a total of $4+4+2 = 10$ spin-zero particles. Three particles are eaten by the gauge bosons and 7 scalars fields are left on the spectrum; two charged Higgs, two 0^- states and three neutral 0^+ states.

The charged Higgs has a mass

$$m_{H_\pm}^2 = 8\left(\lambda_4 v^2 + \frac{c v_\phi^2}{s_{2\beta}}\right). \quad (3.20)$$

In the 0^- sector A_0 and G_ϕ fields mix forming the massless state, the axion:

$$a_\phi = \frac{v s_{2\beta} A_0 + v_\phi G_\phi}{\sqrt{v_\phi^2 + v^2 s_{2\beta}^2}}, \quad (3.21)$$

and the massive state

$$\tilde{A}_0 = \frac{v_\phi A_0 - v s_{2\beta} G_\phi}{\sqrt{v_\phi^2 + v^2 s_{2\beta}^2}}, \quad (3.22)$$

with

$$m_{\tilde{A}_0}^2 = 8c\left(\frac{v_\phi^2}{s_{2\beta}} + v^2 s_{2\beta}\right). \quad (3.23)$$

As was mentioned before, there is mixing in the 0^+ sector. We mark the corresponding 0^+ mass eigenstates as h_i. The mass matrix can be diagonalized in the limit of large v_ϕ, which is astrophysically constrained to be at least of order 10^7 GeV. So, we make an expansion in v/v_ϕ to the second order to get the masses [11]:

$$m_{h_1}^2 = 32v^2\left(\lambda_1 c_\beta^4 + \lambda_2 s_\beta^4 + \lambda_3\right) - 16v^2\frac{\left(a c_\beta^2 + b s_\beta^2 - c s_{2\beta}\right)^2}{\lambda_\phi} \quad (3.24)$$

$$m_{h_2}^2 = \frac{8c}{s_{2\beta}}v_\phi^2 + 8v^2 s_{2\beta}^2(\lambda_1+\lambda_2) - 4v^2\frac{\left[(a-b)s_{2\beta} + 2c c_{2\beta}\right]^2}{\lambda_\phi - \frac{2c}{s_{2\beta}}} \quad (3.25)$$

$$m_{h_3}^2 = 4\lambda_\phi v_\phi^2 + 4v^2 \frac{[(a-b)s_{2\beta} + 2cc_{2\beta}]^2}{\lambda_\phi - \frac{2c}{s_{2\beta}}} + 16v^2 \frac{\left(ac_\beta^2 + bs_\beta^2 - cs_{2\beta}\right)^2}{\lambda_\phi} \tag{3.26}$$

We observe that m_{h_1} is the lightest state, because it is of order v^2 while two other states are of order v_ϕ^2. h_1 is identified with the scalar boson of mass 126 GeV observed at the LHC.

In the paper [11] it is argued that the nominal expansion in powers of v/v_ϕ is applicable in the following cases.

Case 1: The couplings $a,\ b$ and c are generically of $\mathcal{O}(1)$,

Case 2: $a,\ b$ or c are of $\mathcal{O}(v/v_\phi)$,

Case 3: $a,\ b$ or c are of $\mathcal{O}(v^2/v_\phi^2)$ but $c \gg \lambda_i v^2/v_\phi^2$,

If $c \ll \lambda_i v^2/v_\phi^2$ the 0^- state is lighter than the lightest 0^+ Higgs and this case is therefore already phenomenologically unacceptable. The only other case that deserves a separate discussion is

Case 4: Same as in case 3 but $c \sim \lambda_i v^2/v_\phi^2$.

In this case, up to order $\frac{v^2}{v_\phi^2}$, ρ is a mass eigenstate with mass $m_{h_3}^2 = 4\lambda_\phi v_\phi^2$. The two remaining masses are

$$m_{h_1,h_2}^2 = 8v^2 \left(K \mp \sqrt{K^2 - L}\right), \tag{3.27}$$

where

$$\begin{aligned} K &= 2\left(\lambda_1 c_\beta^2 + \lambda_2 s_\beta^2 + \lambda_3\right) + \frac{\bar{c}}{2s_{2\beta}} \\ L &= 8\left[\left(\lambda_1\lambda_2 + \lambda_1\lambda_3 + \lambda_2\lambda_3\right) s_{2\beta}^2 + \frac{\bar{c}}{2s_{2\beta}}\left(\lambda_1 c_\beta^4 + \lambda_2 s_\beta^4 + \lambda_3\right)\right], \\ &\text{with} \quad \bar{c} = \frac{v_\phi^2}{v^2} c. \end{aligned} \tag{3.28}$$

The rotation matrix R from Appendix A is simplified to:

$$R = \begin{pmatrix} \cos\theta & -\sin\theta & 0 \\ \sin\theta & \cos\theta & 0 \\ 0 & 0 & 1 \end{pmatrix}, \tag{3.29}$$

where

$$\tan 2\theta = -\frac{\left(\lambda_1 c_\beta^2 - \lambda_2 s_\beta^2\right) s_{2\beta}}{\left(\lambda_1 c_\beta^2 - \lambda_2 s_\beta^2\right) c_{2\beta} + \lambda_3 + \frac{\bar{c}}{4s_{2\beta}}}. \tag{3.30}$$

The case 1 represents extreme decoupling, when the only light states are h_1, the gauge sector and the axion and all other masses are of order v_ϕ. Case 2 has the similar light content but with the typical scale of heavy particles $\sqrt{v_\phi v}$, that can be the region of hundreds TeV. Cases 3 and 4 can provide much richer phenomenology with h_2, charged Higgs and $\tilde{A}_0$ at the weak scale. One can notice that the presence of these light states requires that some couplings are rather small which my seem odd or fine-tuned. For a discussion on the 'naturalness' of this possibility see [12].

CHAPTER 4

Calculation of oblique corrections

4.1 Definitions and experimental measurements

If the new physics scale is significantly higher than the electroweak scale, new physics effects from virtual particles in loops are expected to contribute predominantly through vacuum polarization corrections to the electroweak precision observables.

One can parametrize possible departures from the SM with the so-called oblique parameters. In our calculations we use the parameters $\epsilon_1,\ \epsilon_2,$ and ϵ_3 defined in [13] as follows:

$$\epsilon_1 \equiv \frac{1}{M_W^2}\left[A^{33}(0) - A^{11}(0)\right], \tag{4.1}$$

$$\epsilon_2 = F^{11}(M_W^2) - F^{33}(M_W^2), \tag{4.2}$$

$$\epsilon_3 = \frac{c}{s}F^{30}(M_Z^2). \tag{4.3}$$

A^{ij} and F^{ij} are the coefficients in the vacuum-polarization tensors

$$\Pi^{ij}_{\mu\nu}(q) = -ig_{\mu\nu}\left[A^{ij}(0) + q^2 F^{ij}(q^2)\right] + q_\mu q_\nu \text{ terms}, \tag{4.4}$$

where ij may be either $WW,\ W_3W_3$ or W_3B and q_μ is the four-momentum of the gauge boson. It is assumed that the term at $g_{\mu\nu}$ can be represented as a series in q^2 because of the new physics scale being much higher then the Fermi scale.

In the effective theory $\epsilon_1,\ \epsilon_2,$ and ϵ_3 receive one-loop contributions from the leading $\mathcal{O}(p^2)$ term and the tree-level contributions from the $a_i(0)$. Thus

$$\epsilon_1 = 2a_0(0) + \dots\,,\ \epsilon_2 = -g^2 a_8(0) + \dots\,,\ \epsilon_3 = -g^2 a_1(0) + \dots\,, \tag{4.5}$$

where the ellipses symbolize the one-loop $\frac{v^2}{4}\,\mathrm{Tr}\,D_\mu\mathcal{U}^\dagger D^\mu\mathcal{U}$ contributions.

Experimental constraints on the oblique parameters are obtained from the global fits of the electroweak sector of the SM. For a long time, such fits have been used to exploit measurements of electroweak precision observables at lepton colliders (LEP, SLC), together with measurements at hadron colliders (Tevatron, LHC), and accurate theoretical predictions at multi-loop level, to constrain free parameters of the SM, such as the Higgs and top masses. Today, all fundamental SM parameters entering these fits are experimentally determined, including information on the Higgs couplings, and the global fits are used as powerful tools to assess the validity of the theory and to constrain scenarios for new physics.

In such papers with global fits [14], [1] it is more common to work with another set of parameters $S,\ T$ and U determined firstly in [15]. The connection of $S,\ T$ and U defined relative to the SM ($\Delta T = T - T^{SM}$, *etc.*) to ϵ_i is as follows:

$$\Delta T = \frac{\epsilon_1 - \epsilon_1^{SM}}{\alpha}, \qquad (4.6)$$

$$\Delta U = -\frac{4s_W^2(\epsilon_2 - \epsilon_2^{SM})}{\alpha}, \qquad (4.7)$$

$$\Delta S = \frac{4s_W^2(\epsilon_3 - \epsilon_3^{SM})}{\alpha}. \qquad (4.8)$$

Here, $\alpha = e^2/(4\pi) = g^2 s_W^2/(4\pi)$ is the fine-structure constant, $s_W = \sin\theta_W$ is the sine of the weak mixing angle θ_W. The ϵ_1 or T parameters are directly connected to the ρ parameter defined in Eqn. (2.2) [13]:

$$\epsilon_1 = \alpha T = \rho. \qquad (4.9)$$

The experimental determinations of $\Delta S,\ \Delta T$ and ΔU from the Gfitter group [14] are

$$\Delta S = 0.05 \pm 0.11, \quad \Delta T = 0.09 \pm 0.13, \quad \Delta U = 0.01 \pm 0.11. \qquad (4.10)$$

The Particle Data Group paper [1] on EW measurements is a year older than the referred one of the Gfitter group. They have slightly different input parameters for the global fits. This results in different values of oblique parameters:

$$\Delta S = -0.03 \pm 0.10, \quad \Delta T = 0.01 \pm 0.12, \quad \Delta U = 0.05 \pm 0.10. \qquad (4.11)$$

ΔU is considered to be very small in most new physics models and therefore often set to zero in the global fits. This changes the experimental limits on $\Delta S,\ \Delta T$ a bit due to correlations between the parameters. The relevant constraints in the $\Delta U = 0$ scenario are [14]:

$$\Delta S|_{\Delta U=0} = 0.06 \pm 0.09, \quad \Delta T|_{\Delta U=0} = 0.1 \pm 0.07. \qquad (4.12)$$

4.2 Diagrams and Feynman Rules

The Feynman diagrams which contribute to the vacuum polarization in the DFSZ model are depicted in Fig. 4.1. There are several types of diagrams:

(a) The gauge-boson line splits into two scalar lines which later reunite to form a new gauge-boson line. Diagrams of this kind constitute a majority in all ϵ_i.

(b) A neutral scalar branches off from the gauge-boson line and loops to a later point in that gauge-boson line.

(c) A scalar branches off from the gauge-boson line and loops back to the same point in that gauge-boson line. This diagram is independent of q^2 and can possibly contribute only in ϵ_1; but in fact it vanishes due to the subtraction in Eq. (4.1).

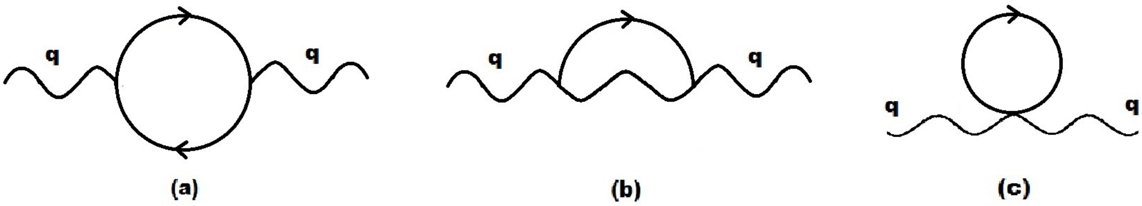

Figure 4.1: Types of Feynman diagrams occurring in the calculation of the vacuum polarizations.

⊸ Tadpole Feynman diagrams also yield a vanishing contribution to ϵ_i.

In Appendix B we provide the details of the computation of diagrams (a) and (b) with arbitrary fields inside a loop.

In our particular model we need to consider the kinetic term (3.9) to get all the interactions. Then, we are able to list all relevant variants of fields inside a loop (different (X, Y) pairs) for different vacuum-polarization tensors. Also, the coefficients γ_{XY} in the numerator of the corresponding integral (see Appendix B) are produced in the following tables:

For $\Pi^{33}(q)$:

X	Y	**Interaction term**	γ_{XY} **coefficient**
H_1	H_2	$\frac{i}{2} g W_3^\alpha H_1 \overleftrightarrow{\partial}_\alpha H_2$	$-\frac{g^2}{4}(2p+q)_\mu(2p+q)_\nu \to -g^2 p_\mu p_\nu$
S	$\tilde{A}_0$	$\frac{g}{2}\frac{v_\phi}{\sqrt{v_\phi^2+v^2 s_{2\beta}^2}} W_3^\alpha S \overleftrightarrow{\partial}_\alpha \tilde{A}_0$	$-\frac{g^2}{4}\frac{v_\phi^2}{v_\phi^2+v^2 s_{2\beta}^2}(2p+q)_\mu(2p+q)_\nu \to -g^2 \frac{v_\phi^2}{v_\phi^2+v^2 s_{2\beta}^2} p_\mu p_\nu$
S	a_ϕ	$g\frac{v \sin 2\beta}{\sqrt{v_\phi^2+v^2 s_{2\beta}^2}} W_3^\alpha S \partial_\alpha a_x$	$-g^2 \frac{v^2 \sin^2 2\beta}{v_\phi^2+v^2 s_{2\beta}^2}(p+q)_\mu(p+q)_\nu \to -g^2 \frac{v^2 \sin^2 2\beta}{v_\phi^2+v^2 s_{2\beta}^2} p_\mu p_\nu$
H	G_0	$-g W_3^\alpha H \partial_\alpha G_0$	$-g^2 (p+q)_\mu (p+q)_\nu \to -g^2 p_\mu p_\nu$
G_1	G_2	$\frac{1}{2} g W_3^\alpha G_1 \overleftrightarrow{\partial}_\alpha G_2$	$-\frac{g^2}{4}(2p+q)_\mu(2p+q)_\nu \to -g^2 p_\mu p_\nu$
B_μ	H	$-\frac{1}{2} g g' v H W_3^\mu B_\mu$	$\frac{1}{4}(g g' v)^2 g_{\mu\nu}$

For $\Pi^{11}(q)$:

X	Y	**Interaction term**	γ_{XY} **coefficient**
H_2	S	$\frac{1}{2} g W_1^\alpha S \overleftrightarrow{\partial}_\alpha H_2$	$-\frac{g^2}{4}(2p+q)_\mu(2p+q)_\nu \to -g^2 p_\mu p_\nu$
H_1	$\tilde{A}_0$	$\frac{g}{2}\frac{v_\phi}{\sqrt{v_\phi^2+v^2 s_{2\beta}^2}} W_1^\alpha \tilde{A}_0 \overleftrightarrow{\partial}_\alpha H_1$	$-\frac{g^2}{4}\frac{v_\phi^2}{v_\phi^2+v^2 s_{2\beta}^2}(2p+q)_\mu(2p+q)_\nu \to -g^2 \frac{v_\phi^2}{v_\phi^2+v^2 s_{2\beta}^2} p_\mu p_\nu$
H_1	a_ϕ	$-g\frac{v \sin 2\beta}{\sqrt{v_\phi^2+v^2 s_{2\beta}^2}} W_1^\alpha H_1 \partial_\alpha a_x$	$-g^2 \frac{v^2 \sin^2 2\beta}{v_\phi^2+v^2 s_{2\beta}^2}(p+q)_\mu(p+q)_\nu \to -g^2 \frac{v^2 \sin^2 2\beta}{v_\phi^2+v^2 s_{2\beta}^2} p_\mu p_\nu$
H	G_1	$-g W_1^\alpha H \partial_\alpha G_1$	$-g^2 (p+q)_\mu (p+q)_\nu \to -g^2 p_\mu p_\nu$
G_2	G_0	$\frac{1}{2} g W_1^\alpha G_2 \overleftrightarrow{\partial}_\alpha G_0$	$-\frac{g^2}{4}(2p+q)_\mu(2p+q)_\nu \to -g^2 p_\mu p_\nu$

For $\Pi^{30}(q)$:

X	Y	**Interaction with** W_3	**Interaction with** B_μ	γ_{XY} **coefficient**
H_1	H_2	$\frac{1}{2} g W_3^\alpha H_1 \overleftrightarrow{\partial}_\alpha H_2$	$\frac{1}{2} g' B^\alpha H_1 \overleftrightarrow{\partial}_\alpha H_2$	$-g g' p_\mu p_\nu$
S	$\tilde{A}_0$	$\frac{g}{2}\frac{v_\phi}{\sqrt{v_\phi^2+v^2 s_{2\beta}^2}} W_3^\alpha S \overleftrightarrow{\partial}_\alpha \tilde{A}_0$	$-\frac{g'}{2}\frac{v_\phi}{\sqrt{v_\phi^2+v^2 s_{2\beta}^2}} B^\alpha S \overleftrightarrow{\partial}_\alpha \tilde{A}_0$	$g g' \frac{v_\phi^2}{v_\phi^2+v^2 s_{2\beta}^2} p_\mu p_\nu$
S	a_ϕ	$g\frac{v \sin 2\beta}{\sqrt{v_\phi^2+v^2 s_{2\beta}^2}} W_3^\alpha S \partial_\alpha a_x$	$-g'\frac{v \sin 2\beta}{\sqrt{v_\phi^2+v^2 s_{2\beta}^2}} B^\alpha S \partial_\alpha a_x$	$g g' \frac{v^2 \sin^2 2\beta}{v_\phi^2+v^2 s_{2\beta}^2} p_\mu p_\nu$
H	G_0	$-g W_3^\alpha H \partial_\alpha G_0$	$g' B^\alpha H \partial_\alpha G_0$	$g g' p_\mu p_\nu$
G_1	G_2	$\frac{1}{2} g W_3^\alpha G_1 \overleftrightarrow{\partial}_\alpha G_2$	$\frac{1}{2} g' B^\alpha G_1 \overleftrightarrow{\partial}_\alpha G_2$	$-g g' p_\mu p_\nu$

4.3 Resulting expressions

In this section we write down the exact results in the DFSZ model to the $\delta\epsilon_i$ at one loop, defined as

$$\delta\epsilon_i = \epsilon_i^{DFSZ} - \epsilon_i^{SM}. \tag{4.13}$$

Taking into account that we are interested in deviations with respect to the minimal Standard Model, diagrams with the following pairs in loop (H_1, H_2), (S, $\tilde{A}_0$), (S, a_ϕ), (H, B_μ), (H_2, S), (H_1, $\tilde{A}_0$), (H_1, a_ϕ) make a new contribution to $\delta\epsilon_1$. (H, G_0) pair contains in fact three diagrams, one of which with $R_{h_1}h_1$ overlaps with the SM diagram with a (H_{SM}, G_0) pair. Diagram with (G_1, G_2) pairs cancels exactly with the same in the SM. Then,

$$\begin{aligned}\delta\epsilon_1 = {} & \frac{g^2}{16\pi^2}\frac{1}{4M_W^2}\left(\sum_{i=1}^{3} R_{Si}^2\left(\frac{v_\phi^2}{v_\phi^2+v^2 s_{2\beta}^2} f(m_{\tilde{A}_0}^2, m_{h_i}^2) - f(m_{H_\pm}^2, m_{h_i}^2)\right) + m_{H_\pm}^2 - \right. \\ & \left. - \frac{v_\phi^2}{v_\phi^2+v^2 s_{2\beta}^2} f(m_{H_\pm}^2, m_{\tilde{A}_0}^2)\right) - \frac{g'^2}{16\pi^2}\frac{3}{4M_W^2}\sum_{i=1}^{3} R_{Hi}^2 \ln\frac{m_{h_i}^2}{m_{H_{SM}}^2},\end{aligned} \tag{4.14}$$

here the function f is $f(X,Y) = \frac{XY}{Y-X}\ln\frac{Y}{X}$ for $X \neq Y$ and $f(X,X) = X$.

Considerations of the same kind as for $\delta\epsilon_1$ hold for remaining two oblique parameters. Diagrams with only Goldstone bosons cancel, with one Goldstone boson and H undertake partial cancelation, while other diagrams with pairs listed in tables of the previous section result in new contributions.

$$\begin{aligned}\delta\epsilon_2 = {} & -\frac{g^2}{16\pi^2}\frac{1}{12}\left(\frac{1}{2}\frac{v^2\sin^2 2\beta}{v_\phi^2+v^2 s_{2\beta}^2}\ln\frac{m_{H_\pm}^2}{m_{H_{SM}}^2} + \frac{v_\phi^2}{v_\phi^2+v^2 s_{2\beta}^2} g(m_{H_\pm}^2, m_{\tilde{A}_0}^2) + \right. \\ & \left. + \sum_{i=1}^{3} R_{Si}^2\left(g(m_{H_\pm}^2, m_{h_i}^2) - \frac{1}{2}\frac{v^2\sin^2 2\beta}{v_\phi^2+v^2 s_{2\beta}^2}\ln\frac{m_{h_i}^2}{m_{H_{SM}}^2} - \frac{v_\phi^2}{v_\phi^2+v^2 s_{2\beta}^2} g(m_{\tilde{A}_0}^2, m_{h_i}^2)\right)\right),\end{aligned} \tag{4.15}$$

here the function g is $g(X,Y) = -\frac{5}{6} + \frac{2XY}{(X-Y)^2} + \frac{(X+Y)(X^2-4XY+Y^2)}{2(X-Y)^3}\ln\frac{X}{Y}$.

$$\begin{aligned}\delta\epsilon_3 = {} & \frac{g^2}{16\pi^2}\frac{1}{12}\left(-\ln\frac{m_{H_\pm}^2}{m_{H_{SM}}^2} + \frac{1}{2}\frac{v_\phi^2}{v_\phi^2+v^2 s_{2\beta}^2}\ln\frac{m_{\tilde{A}_0}^2}{m_{H_{SM}}^2} - \frac{5}{6}\frac{v^2\sin^2 2\beta}{v_\phi^2+v^2 s_{2\beta}^2} + \right. \\ & + \sum_{i=1}^{3} R_{Si}^2\left(\frac{v_\phi^2}{v_\phi^2+v^2 s_{2\beta}^2} g(m_{h_i}^2, m_{\tilde{A}_0}^2) + \ln\frac{m_{h_i}^2}{m_{H_{SM}}^2} - \right. \\ & \left.\left. - \frac{1}{2}\frac{v_\phi^2}{v_\phi^2+v^2 s_{2\beta}^2}\ln\frac{m_{h_i}^2}{m_{H_{SM}}^2}\right) + \sum_{i=1}^{3} R_{Hi}^2 \ln\frac{m_{h_i}^2}{m_{H_{SM}}^2}\right)\end{aligned} \tag{4.16}$$

These results are consistent with the ones given in the limit $v_\phi \to \infty$ [8].

Some comments on the calculations should be provided. Firstly, $m_{H_{SM}}^2$ appears in Eqn. (4.14)-(4.16) due to the subtraction of the SM contributions in Eqn. (4.13). As stated previously, $m_{H_{SM}}$ is identified with m_{h_1}. Secondly, we are interested only in the leading corrections in the limit $q^2 \approx M_W^2 \ll M_s$, where M_s is a typical heavy-scalar mass. It means, that we can set masses of gauge and Goldstone bosons equal to zero $M_W = M_G = 0$ in the internal lines. Thus, we use Eqn. (B.22) from Appendix B to derive the contribution of type (b) diagrams from Fig. 4.1.

One more note to the $\delta\epsilon_1$ expression: it is possible to have in Π^{33} pairs $(H,\, B_\mu)$ and $(H,\, W_\mu^3)$ in a loop, while in Π^{11} there is an option of $(H,\, W_\mu^1)$ in a loop. Terms with W_μ cancel each other, and the one with B_μ gives a term proportional to g' in Eqn. (4.14).

Furthermore, when calculating the diagrams contributing to $\delta\epsilon_2$ and $\delta\epsilon_3$, those with gauge bosons in the internal lines do not contribute. These simplifications follow from explicit form of the corresponding contribution (see Eqn. (B.21)) and also from simple dimensional considerations. For instance, the diagrams containing one internal vector-boson line are proportional to $g^2 M_W^2$ and their overall contribution to $\delta\epsilon_3$ is ultraviolet finite. Since $\delta\epsilon_3$ is proportional to the dimensionless derivatives of the vacuum polarization, there must be a M_s^2 in the denominator, and so the contribution is proportional to M_W^2/M_s^2 and, therefore, subleading. This is the reason there is no g' term in $\delta\epsilon_2$ and no contribution from type (b) diagrams in $\delta\epsilon_3$.

CHAPTER 5

Spectrum implications

5.1 Custodial and Quasi-Custodial limits

Consider the case of $SU(2)_L \times SU(2)_R$ global symmetry being spontaneously broken to $SU(2)_V$. In this case, the VEVs of the Higgs doublets are equal and $\tan\beta = 1$. The masses are:

$$m^2_{H_\pm} = 8(2\lambda v^2 + c v_\phi^2), \quad m^2_{\tilde{A}_0} = 8c(v^2 + v_\phi^2), \text{ and } m^2_{h_2} = m^2_{H_\pm}, \tag{5.1}$$

$$m^2_{h_1} = 16v^2\left(\lambda + 2\lambda_3 - \frac{(a-c)^2}{\lambda_\phi}\right) \text{ and } m^2_{h_3} = 4\left(\lambda_\phi v_\phi^2 + 4v^2\frac{(a-c)^2}{\lambda_\phi}\right). \tag{5.2}$$

We can explore what range of masses is allowed by the experimental determinations of oblique parameters in this relatively simple case. As we are basically interested in the possibility of obtaining a lightish spectrum, we discuss the case 4 of the Chapter 3 where the c parameter scales as v^2/v_ϕ^2. Hence, the rotation matrix of 0^+ states is equal to unity. All $\delta\epsilon_i$ depend only on $m_{H_\pm} = m_{h_2}$ and $m_{\tilde{A}_0}$; we also use $m_{h_1} = 125$ GeV. Moreover, we have to require the stability of the potential discussed in Appendix C.

The custodial symmetry gives us $\Delta T = 0$ automatically. The ΔU experimental value puts a rather high upper bound (in multi TeV region) to the spectrum of charged Higgses. Taken as it is given in papers (see Eqn. (4.10), (4.11)) ΔS would not pose any restrictions. However, it is interesting to notice that the center value $\Delta S = 0.05$ lies in the region forbidden by the stability requirements. Only when a positive ΔS comes very close to 0 some spectrum can exist as it is shown on Figure 5.1. If $\Delta S < 0$ the masses to the left from the diagonal become allowed.

Now, let us assume a 'quasi-custodial' setting which means that the custodial symmetry is broken only via the coupling $\lambda_{4B} = \lambda_4 - 2\lambda$ being non-zero. The mass spectrum stays the same but for

$$m^2_{H_\pm} = m^2_{h_2} + 8v^2\lambda_{4B}. \tag{5.3}$$

The range of masses allowed by the present constraints on ΔS for different values of λ_{4B} is shown in Figure 5.2. The negative values of λ_{4B} allow much lighter spectra than the positive ones. This can also be seen in Figure 5.3 where we depict constraints both from ΔS and ΔT. ΔT significantly narrows the allowed region, while ΔU gives nothing new. For $\lambda_{4B} = 0.2$ the possible range starts at about 1 TeV range, while for negative λ_{4B} it goes down to 100 GeV.

5.2 General case

In this section we completely give up the custodial symmetry and consider the general case 4. Hence, the three masses $m_{\tilde{A}_0}$, $m_{H_\pm}$ and m_{h_2} are unrelated, except for the eventual lack of

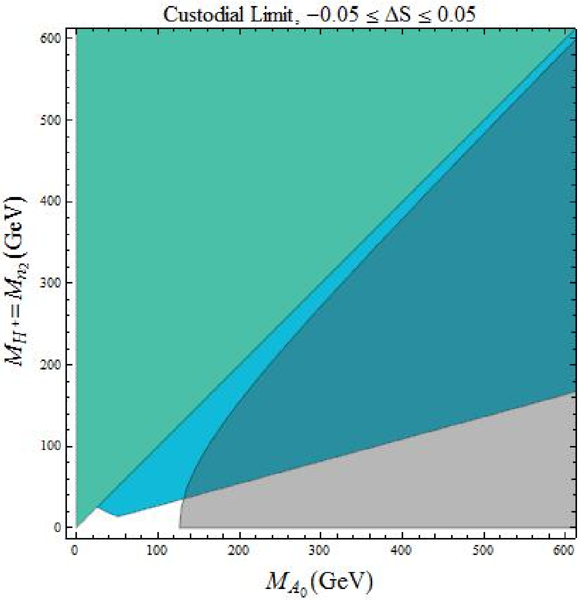

Figure 5.1: $0 \leq \Delta S \leq 0.05$, blue; $-0.05 \leq \Delta S \leq 0$, green. Grey regions: excluded by stability.

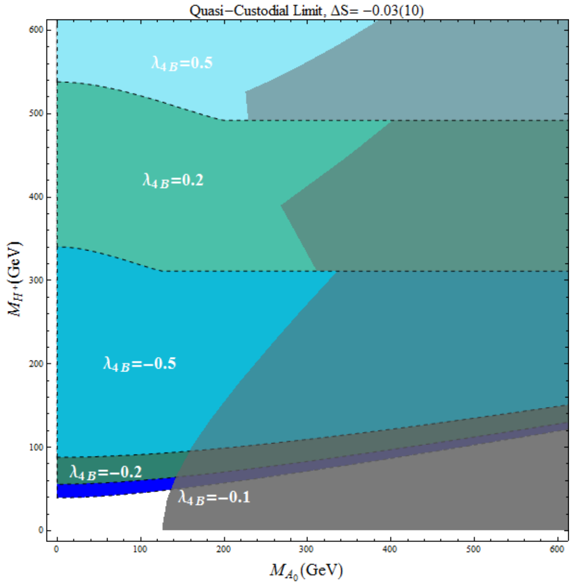

Figure 5.2: ΔS in the quasi-custodial limit for different values of the symmetry breaking parameter λ_{4B}.

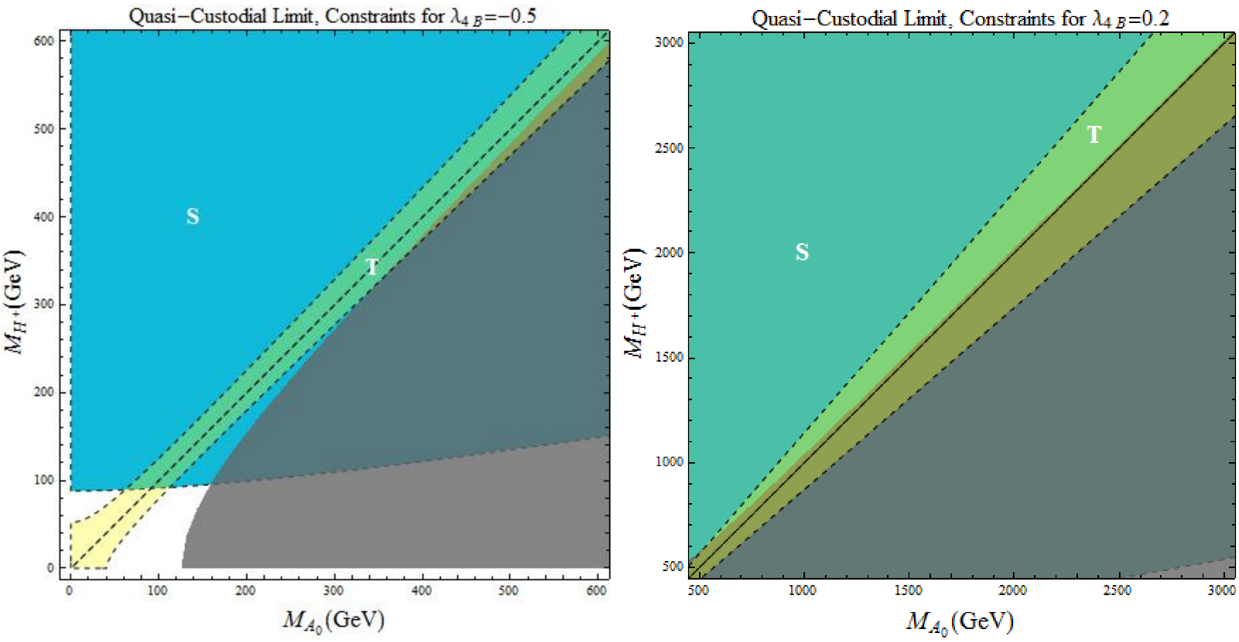

Figure 5.3: Restrictions in the quasi-custodial limit for different values of λ_{4B}. Allowed regions: ΔT (yellow) overlaps ΔS (blue or green) excluding grey areas forbidden by stability.

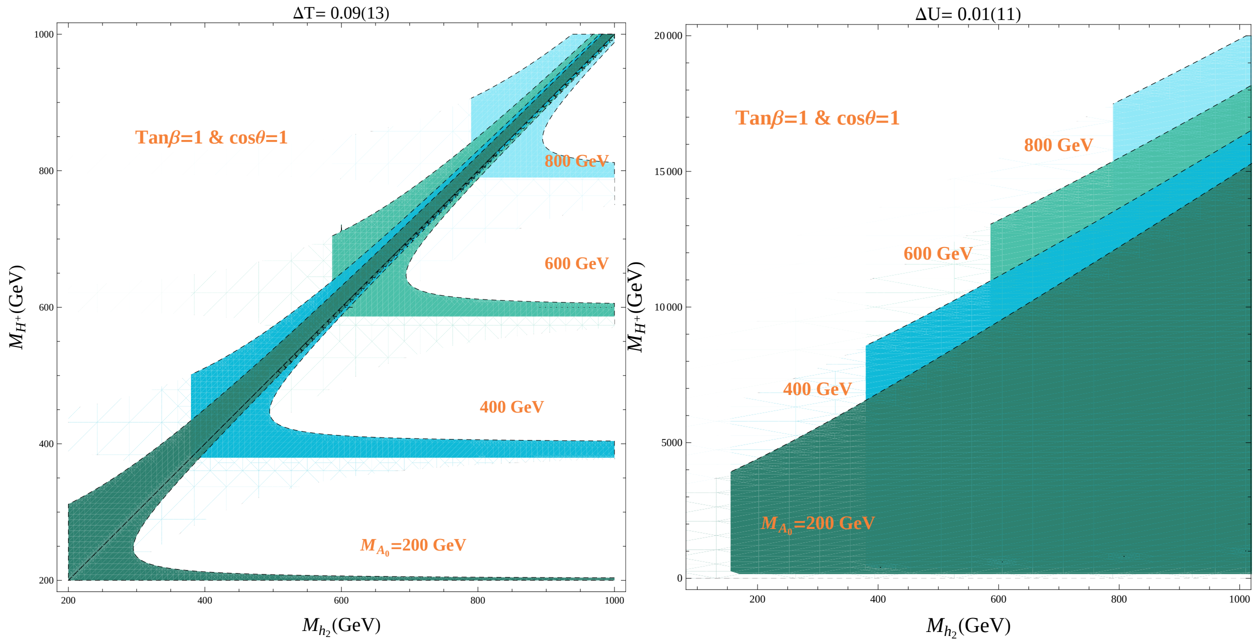

Figure 5.4: Exclusion plots imposed by the constraint from ΔT (left) and ΔU (right) on the h_2 and $H_{\pm}$. The successive horizontal bands correspond to different values of m_{A_0}. The stability bounds are implemented.

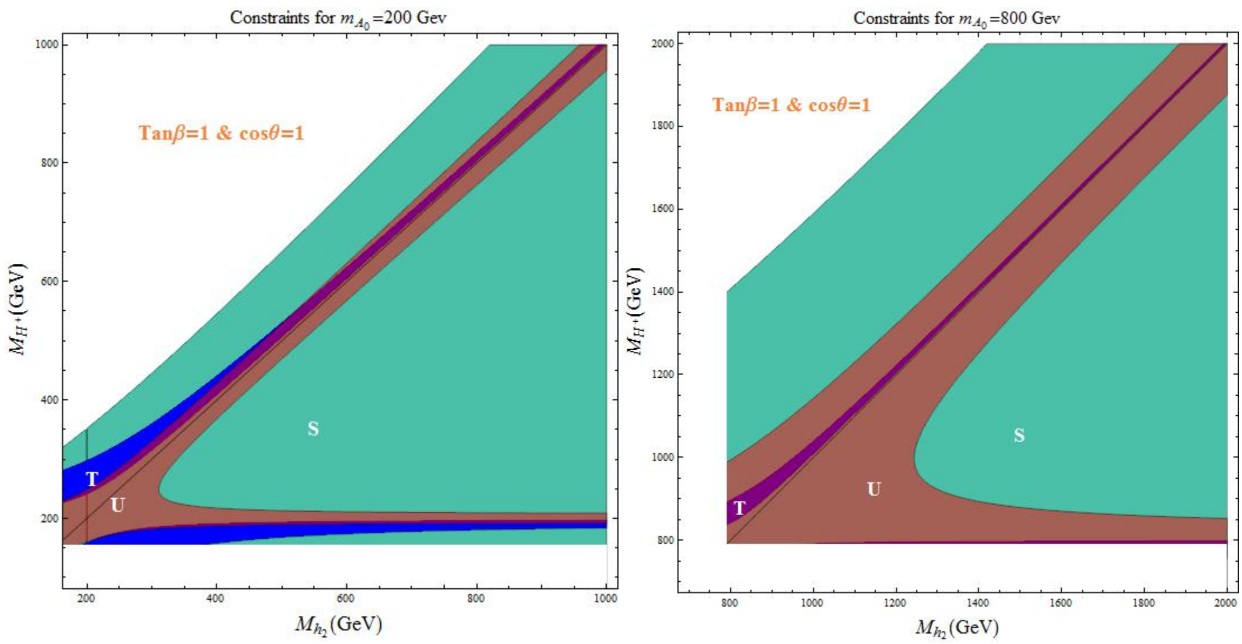

Figure 5.5: Exclusion plots imposed by the simultaneous constraints from ΔT, ΔS, $\Delta U \simeq 0$ and requirement of stability on the h_2 and $H_{\pm}$. The left plot corresponds to $m_{A_0} = 200$ GeV the right one to $m_{A_0} = 800$ GeV.

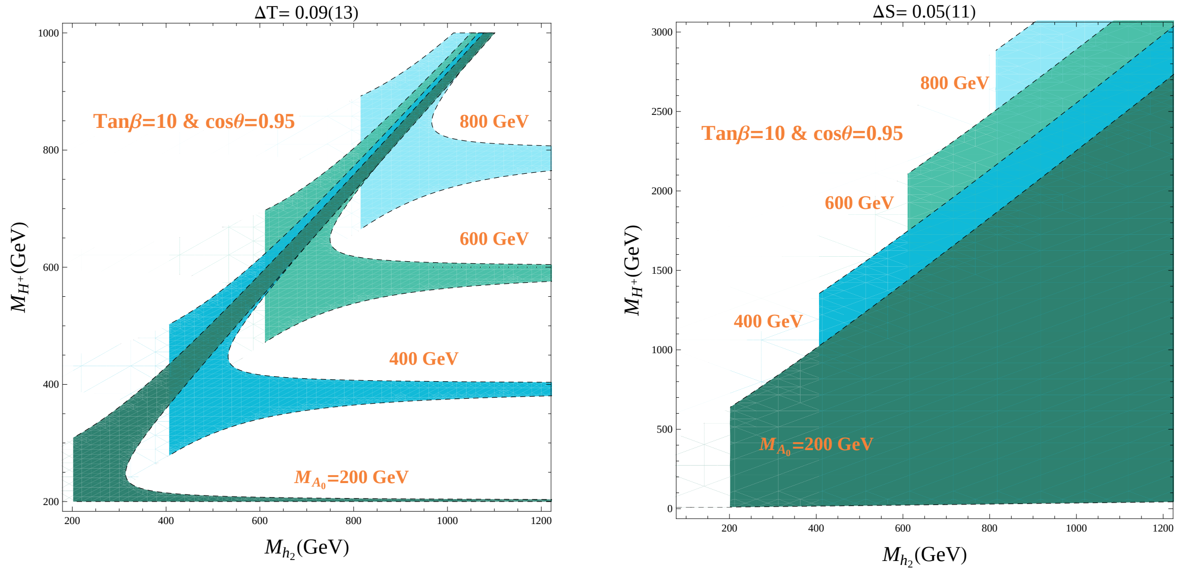

Figure 5.6: Exclusion plots imposed by the constraint from ΔT (left) and ΔS (right) on the h_2 and $H_\pm$ for $\tan\beta = 10$ and $\cos\theta = 0.95$

stability of the potential. In this case, the rotation matrix R can be different form the identity. In particular, the angle θ from Eqn. (3.30) may be not vanishing. However, experimentally $\cos\theta$ is known [11] to be very close to one.

If we assume that $\cos\theta$ is exactly equal to one, we can get the exclusion/acceptance regions for all oblique parameters. ΔT gives manifestly larger constraint than two other parameters; constraints from ΔT and ΔU are depicted in Fig. 5.4. However, it is commonly agreed that ΔU should be very small. It is zero in the SM and lots of global electroweak fits are done under this condition. Posing $\Delta U \simeq 0$ we get much smaller allowed region than the one in Fig. 5.4 (right). Thus, we plot in Fig. 5.5 areas allowed by all three parameters simultaneously within the $\Delta U = 0$ scenario to see where they cross. As ΔU gets closer to exact zero its region shrinks to two lines, which overlap with ΔT region only asymptotically at infinity.

Another choice of angles β and θ is also possible. In general 2HDMs a quite large range of $\tan\beta$ can be considered. For $\cos\theta$ values from 0.9 to 1 are still allowed by existing constraints. In Fig 5.6 there are plots depicting constraints ΔT and ΔS put on the spectrum in case of $\tan\beta = 10$ and $\cos\theta = 0.95$.

CHAPTER 6

Conclusions

The nature of electroweak symmetry breaking keeps being an important issue in particle physics today. The Standard Model of particle physics contains a mechanism for electroweak symmetry breaking, and the discovery of the Higgs boson at the LHC proves its consistency. However, the Minimal Standard Model still has a several well-known problems. One of them being the absence of degree of freedom for dark matter.

Other models with a similar electroweak symmetry breaking pattern can be proposed. In this thesis we study the Dine-Fischler-Srednicki-Zhitnitsky model, an extension of the 2HDM. It also contains an invisible axion which is an interesting candidate for dark matter. Being extremely weakly coupled the axion cannot be directly detected at the LHC. Hence, we make an investigation what indirect consequences of the axion presence can be seen experimentally.

The Peccei-Quinn symmetry, responsible for the appearance of an axion, restricts the form of the effective potential. Further, we include the constraints from electroweak precision parameters expressed in values of the oblique parameters. Current experimental limits on the oblique parameters agree with the SM predictions well enough. Now there is a room for the new physics also, but the refinement of experimental measurements can be even more in favour of the SM.

The large scale, appearing in the DFSZ model to make the axion nearly invisible, seems to generate a very heavy and inaccessible spectrum of the new physics. However, we discuss cases in which a rather light spectrum appears, with even a possibility to be tested at the LHC. This requires some specific couplings to be very small, which has been argued [12] to be technically natural, as the couplings in question do break some extended symmetry and are therefore protected. This lightish spectrum is severely constrained, making it easier to prove or disprove such prediction in the near future.

Bibliography

[1] K.A. Olive et al. (Particle Data Group), Chin. Phys. C, 38, 090001 (2014).

[2] G. C. Branco, P. M. Ferreira, L. Lavoura, M. N. Rebelo, M. Sher and J. P. Silva, Phys. Rept. 516, 1 (2012) [arXiv:1106.0034 [hep-ph]].

[3] R. D. Peccei and H. R. Quinn, Phys. Rev. Lett. 38 (1977) 1440; Phys. Rev. D16 (1977) 1791.

[4] S. Weinberg, Phys. Rev. Lett. 40 (1978) 223; F. Wilczek, Phys. Rev. lett. 40 (1978) 279.

[5] M. Dine, W. Fischler and M. Srednicki, Phys. Lett. B, 104, 199 (1981).

[6] A.R. Zhitnitsky, Sov. J. Nucl. Phys. 31 (1980) 260 [Yad. Fiz.31(1980) 497].

[7] M. Kuster, G. Raffelt and B. Beltran (eds), Lecture Notes in Physics 741 (2008).

[8] P. Ciafaloni and D. Espriu, Phys. Rev. D 56, 1752 (1997) [hep-ph/9612383].

[9] A. Pomarol and R. Vega, Nucl.Phys. B413 (1994) 3; B. Grzadkowski, M. Maniatis and J. Wudka (UC, Riverside), JHEP 1111 (2011) 030.

[10] R.L. Delgado, A. Dobado and F. J. Llanes-Estrada, JHEP 1402 (2014) 121; arXiv:1408.1193; arXiv:1502.04841; D. Espriu, F. Mescia and B. Yencho, Phys. Rev. D 88, 055002 (2013) [arXiv:1307.2400 [hep-ph]].

[11] D. Espriu, F. Mescia and A. Renau, arXiv:1503.0295 [hep-ph].

[12] R. R. Volkas, A. J. Davies and G. C. Joshi, Phys. Lett. B 215, 133 (1988); R. Foot, A. Kobakhidze, K. L. McDonald and R. R. Volkas, Phys. Rev. D 89, no. 11, 115018 (2014) [arXiv:1310.0223 [hep-ph]].

[13] G. Altarelli and R. Barbieri, Phys. Lett. B 253, 161 (1990).

[14] M. Baak, J. Cuth, J. Hallec, A. Hoecker, R. Kogler, K. Monig, M. Schott, J. Stelzer, Eur. Phys. J. C (2014) 74:3046 [arXiv:1407.3792v1 [hep-ph]].

[15] M. Peskin and T. Takeuchi, Phys. Rev. Lett. 65, 1964 (1990).

[16] J. F. Gunion and H. E. Haber, Phys. Rev. D 67, 075019 (2003) [hep-ph/0207010].

APPENDIX A

The 3×3 0^+ neutral scalar mass matrix

The 3×3 neutral scalar mass matrix is

$$M_{HS\rho} = 4 \begin{pmatrix} 8v^2 \left(\lambda_1 c_\beta^4 + \lambda_2 s_\beta^4 + \lambda_3\right) & 4v^2 \left(-\lambda_1 c_\beta^2 + \lambda_2 s_\beta^2\right) s_{2\beta}^2 & 2vv_\phi \left(ac_\beta^2 + bs_\beta^2 + cs_{2\beta}\right) \\ 4v^2 \left(-\lambda_1 c_\beta^2 + \lambda_2 s_\beta^2\right) s_{2\beta}^2 & -\frac{2cv_\phi^2}{s_{2\beta}} + 2v^2 \left(\lambda_1 + \lambda_2\right) s_{2\beta}^2 & vv_\phi \left[\left(-a+b\right) s_{2\beta} + 2cc_{2\beta}\right] \\ 2vv_\phi \left(ac_\beta^2 + bs_\beta^2 + cs_{2\beta}\right) & vv_\phi \left[\left(-a+b\right) s_{2\beta} + 2cc_{2\beta}\right] & \lambda_\phi v_\phi^2 \end{pmatrix}. \tag{A.1}$$

This matrix can be diagonalized with a rotation

$$\begin{pmatrix} H \\ S \\ \rho \end{pmatrix} = R \begin{pmatrix} h_1 \\ h_2 \\ h_3 \end{pmatrix} \tag{A.2}$$

We write the rotation matrix as

$$R = \exp\left(\frac{v}{v_\phi} A + \frac{v^2}{v_\phi^2} B\right), \quad A^T = -A, \quad B^T = -B \tag{A.3}$$

and work up to the second order in $\frac{v}{v_\phi}$. It can be shown [11] that

$$A_{12} = B_{13} = B_{23} = 0, \tag{A.4}$$

so the matrix is

$$R = \begin{pmatrix} 1 - \frac{v^2}{v_\phi^2} \frac{A_{13}^2}{2} & -\frac{v^2}{v_\phi^2} \frac{A_{13}A_{23} - 2B_{12}}{2} & \frac{v}{v_\phi} A_{13} \\ -\frac{v^2}{v_\phi^2} \frac{A_{13}A_{23} + 2B_{12}}{2} & 1 - \frac{v^2}{v_\phi^2} \frac{A_{23}^2}{2} & \frac{v}{v_\phi} A_{23} \\ -\frac{v}{v_\phi} A_{13} & -\frac{v}{v_\phi} A_{23} & 1 - \frac{v^2}{v_\phi^2} \frac{A_{13}^2 + A_{23}^2}{2} \end{pmatrix}, \tag{A.5}$$

with

$$A_{13} = \frac{2}{\lambda_\phi} \left(ac_\beta^2 + bs_\beta^2 + cs_{2\beta}\right), \; A_{23} = \frac{(-a+b)s_{2\beta} + 2cc_{2\beta}}{\lambda_\phi + \frac{2c}{s_{2\beta}}}, \tag{A.6}$$

$$B_{12} = \frac{2}{c} s_{2\beta}^2 \left(\lambda_1 c_\beta^2 - \lambda_2 s_\beta^2\right) + \frac{s_{2\beta}}{\lambda_\phi c} \frac{c + \lambda_\phi s_{2\beta}}{2c + \lambda_\phi s_{2\beta}} \left(ac_\beta^2 + bs_\beta^2 + cs_{2\beta}\right) \left[(-a+b)s_{2\beta} + 2cc_{2\beta}\right]. \tag{A.7}$$

APPENDIX B

Integrals

In the text we define the vacuum-polarization tensors as:

$$\Pi^{ij}_{\mu\nu}(q) = -ig_{\mu\nu}\left[A^{ij}(0) + q^2 F^{ij}(q^2)\right] + q^\mu q^\nu \text{ terms.} \tag{B.1}$$

B.1 Loops with two scalars

Consider the diagram in Fig. B.1. The momentum of the gauge boson is q; p is the momentum of the X particle, entering the first vertex, and the particle Y has momentum $p+q$ going into the second vertex.

These diagrams produce three kinds of terms. The terms proportional to two powers of the external momentum, $q_\mu q_\nu$, do not enter in A^{ij}. The terms proportional to just one power, $q_\mu p_\nu$ and $p_\mu q_\nu$, vanish when integrated. The terms containing only the momentum running in the loop, $p_\mu p_\nu$, are the ones we are interested in

After removing the q_μ pieces, each diagram contributes

$$I^{\mu\nu} = -\gamma_{XY}\mu^\epsilon \int \frac{d^dp}{(2\pi)^d} \frac{p^\mu p^\nu}{[p^2 - m_X^2 + i\epsilon]\,[(p+q)^2 - m_Y^2 + i\epsilon]}, \tag{B.2}$$

where γ_{XY} is the coefficient in front of $p_\mu p_\nu$ in the Feynman Rule for the two vertices of the diagram. Using Feynman parameters,

$$I^{\mu\nu} = -\gamma_{XY}\mu^\epsilon \int_0^1 dz \int \frac{d^dk}{(2\pi)^d} \frac{k^\mu k^\nu}{(k^2 - C + i\epsilon)^2}, \quad C = z(z-1)q^2 + m_X^2(1-z) + m_Y^2 z, \tag{B.3}$$

(as usual, we have redefined the variable in the integral $k = p + zq$ and thrown away q^μ and $q^\mu q^\nu$ terms). Taking the k integral with $n = 2$, we get:

$$I^{\mu\nu} = -\frac{ig^{\mu\nu}}{32\pi^2}\gamma_{XY} \int_0^1 dz\,\left[(1 + \Delta_\epsilon + \ln\mu^2)C - C\log C\right], \tag{B.4}$$

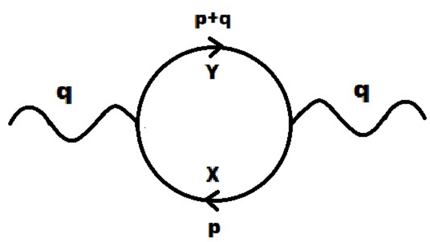

Figure B.1: A diagram with two scalars in a loop.

where $\Delta_\epsilon \equiv \frac{2}{\epsilon} - \gamma + \log 4\pi$. The first integral is just

$$\int_0^1 dz C = \frac{1}{2}\left(-\frac{q^2}{3} + m_X^2 + m_Y^2\right). \tag{B.5}$$

The second one is easy to compute when $q^2 = 0$:

$$\int_0^1 dz(-C\log C)\Big|_{q^2=0} = \frac{m_X^2 + m_Y^2}{4} - \frac{m_X^4 \log(m_X^2) - m_Y^4 \log(m_Y^2)}{2(m_X^2 - m_Y^2)}. \tag{B.6}$$

The general expression for the integral (B.2) is much more complicated but can be obtained exactly:

$$I^{\mu\nu}(Q) = -\frac{ig^{\mu\nu}}{32\pi^2}\gamma_{XY}\left(\left(1 + \Delta_\epsilon - \frac{1}{2}\ln\frac{I}{\mu^2} - \frac{1}{2}\ln\frac{J}{\mu^2}\right)\left(-\frac{Q}{6} + \frac{I+J}{2}\right) + \frac{2}{3}(I+J) - \frac{5}{18}Q - \right.$$
$$\left. - \frac{(I-J)^2}{6Q} + \left(\frac{(I-J)^2}{3Q} - I - J\right)\frac{I-J}{4Q}\ln\frac{I}{J} + \frac{r}{12Q^2}f(t,r)\right). \tag{B.7}$$

Here $I = m_X^2$, $J = m_Y^2$, $Q = q^2$, $r = Q^2 - 2Q(I+J) + (I-J)^2$, $t = I + J - Q$, and

$$f(t,r) = \begin{cases} \sqrt{r}\ln\left|\frac{t-\sqrt{r}}{t+\sqrt{r}}\right| & r > 0 \\ 0 & r = 0 \\ 2\sqrt{-r}\arctan\frac{\sqrt{-r}}{t} & r < 0 \end{cases}$$

Expanding (B.7) in Q we arrive at Q^0 to the expression of A^{ij}:

$$A^{ij}_{I,J} = \frac{\gamma_{XY}}{64\pi^2}\left(\left(\frac{3}{2} + \Delta_\epsilon\right)(I+J) - \frac{I^2\ln\frac{I}{\mu^2} - J^2\ln\frac{J}{\mu^2}}{I-J}\right), \tag{B.8}$$

which can be rewritten as:

$$A^{ij}_{I,J} = \frac{\gamma_{XY}}{64\pi^2}\left((1+\Delta_\epsilon)(I+J) - I\ln\frac{I}{\mu^2} - J\ln\frac{J}{\mu^2} + f(I,J)\right), \tag{B.9}$$
$$\text{where } f(I,J) = \frac{1}{2}(I+J) + \frac{IJ}{I-J}\ln\frac{J}{I}.$$

For $I = J$ we have $f(I,I) = 2I$ and

$$A^{ij}_{I=J} = \frac{\gamma_{XY}}{32\pi^2}\left((1+\Delta_\epsilon)I - I\ln\frac{I}{\mu^2} + I\right). \tag{B.10}$$

If one of the masses goes to zero $I = 0$:

$$A^{ij}_{I=0,J} = \frac{\gamma_{XY}}{64\pi^2}\left((1+\Delta_\epsilon)J - J\ln\frac{J}{\mu^2} + J/2\right). \tag{B.11}$$

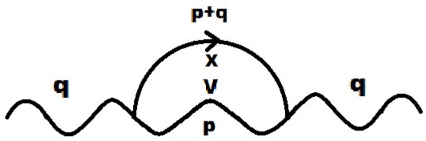

Figure B.2: A diagram with a scalar and a vector particle in a loop.

In the Q^1 order we get the expression of $F^{ij}(0)$

$$F^{ij}_{I,J} = \frac{1}{32\pi^2}\gamma_{XY}\frac{1}{6}\left(-\frac{5}{6} - \Delta_\epsilon + \frac{1}{2}\ln\frac{I}{\mu^2} + \frac{1}{2}\ln\frac{J}{\mu^2} + \frac{1}{2}\frac{(I+J)(I^2-4IJ+J^2)}{(I-J)^3}\ln\frac{I}{J} + \frac{2IJ}{(I-J)^2}\right). \tag{B.12}$$

It can be rewritten as:

$$F^{ij}_{I,J} = \frac{1}{16\pi^2}\gamma_{XY}\frac{1}{12}\left(-\Delta_\epsilon + \frac{1}{2}\ln\frac{I}{\mu^2} + \frac{1}{2}\ln\frac{J}{\mu^2} + g(I,J)\right), \tag{B.13}$$

$$\text{where } g(I,J) = -\frac{5}{6} + \frac{2IJ}{(I-J)^2} + \frac{(I+J)(I^2-4IJ+J^2)}{2(I-J)^3}\ln\frac{I}{J}. \tag{B.14}$$

For $I = J$ Eqn. (B.12) is simplified to

$$F^{ij}_{I=J} = \frac{1}{16\pi^2}\gamma_{XY}\frac{1}{12}\left(-\Delta_\epsilon + \ln\frac{I}{\mu^2}\right). \tag{B.15}$$

And for the case of one of the particles (X,Y) being massless Eqn. (B.12) turns into:

$$F^{ij}_{I=0,J} = \frac{1}{16\pi^2}\gamma_{XY}\frac{1}{12}\left(-\frac{5}{6} - \Delta_\epsilon + \ln\frac{J}{\mu^2}\right) \tag{B.16}$$

B.2 Loops with a scalar and a vector particle

We work in the 't Hooft-Feynman gauge $\xi = 1$ and the vector boson propagator has the form:

$$\frac{-i}{k^2 - M_W^2 + i\varepsilon}. \tag{B.17}$$

For the diagram in Fig. B.2 we have the following integral:

$$I^{\mu\nu} = \gamma_{XY}\mu^\epsilon \int \frac{d^dp}{(2\pi)^d}\frac{g^{\mu\nu}}{[p^2 - m_V^2 + i\epsilon]\,[(p+q)^2 - m_X^2 + i\epsilon]}. \tag{B.18}$$

Performing the calculations of the same kind as in the previous section we eventually get:

$$I^{\mu\nu} = \frac{ig^{\mu\nu}}{16\pi^2}\gamma_{XY}\int_0^1 dz\left[\Delta_\epsilon + \ln\mu^2 - \ln C\right]. \tag{B.19}$$

Let us call $I = m_X^2$, $J = m_V^2$. Expansion in Q produces in the general case:

$$A^{ij} = \frac{\gamma_{XY}}{16\pi^2} \left(-\Delta_\epsilon - 1 + \frac{I \ln \frac{I}{\mu^2} - J \ln \frac{J}{\mu^2}}{I - J} \right), \tag{B.20}$$

$$F^{ij} = \frac{\gamma_{XY}}{32\pi^2} \left(\frac{J^2 - I^2}{(I-J)^3} + \frac{2IJ}{(I-J)^3} \left(\ln \frac{I}{\mu^2} - \ln \frac{J}{\mu^2} \right) \right). \tag{B.21}$$

If the vector particle mass can be set equal to zero $J = 0$, we can expand (B.18) in Q as:

$$I^{\mu\nu}_{m_V=0} = -\frac{ig^{\mu\nu}}{16\pi^2} \gamma_{XY} \left[-\Delta_\epsilon - \ln \mu^2 - 1 + \ln I - \frac{Q}{2I} \right]. \tag{B.22}$$

APPENDIX C

Vacuum stability conditions and mass relations

Following the work [16] we note that vacuum stability (the fact that the potential does not go to $-\infty$ or 0 for any direction in the fields) imposes the following conditions on the parameters of the potential:

$$\lambda_1+\lambda_3>0, \quad \lambda_2+\lambda_3>0, \quad 2\lambda_3+\lambda_4+2\sqrt{(\lambda_1+\lambda_3)(\lambda_2+\lambda_3)}>0,$$
$$\lambda_3+\sqrt{(\lambda_1+\lambda_3)(\lambda_2+\lambda_3)}>0. \tag{C.1}$$

In the case of custodial symmetry (keeping the possibility of breaking in λ_4) these conditions reduce to

$$\lambda+\lambda_3>0, \quad \lambda+2\lambda_3>0, \quad 2\lambda+4\lambda_3+\lambda_4>0 \tag{C.2}$$

and they impose two conditions on the masses:

$$m_{A_0}^2+m_{h_1}^2-m_{h_2}^2>0, \quad m_{H_\pm}^2+m_{h_1}^2-m_{A_0}^2>0. \tag{C.3}$$